

Turbulent Boundary Layer Behind Constant Velocity Shock Including Wall Blowing Effects

H. Mirels*

The Aerospace Corporation, El Segundo, California

A theory, previously presented by the author, concerning turbulent boundary-layer development behind a shock moving with uniform speed is used to obtain numerical results for turbulent boundary-layer properties in air. Numerical results are tabulated for shock propagation at Mach numbers in the range $1.01 \leq M_s \leq 20$. The heat-transfer results are in good agreement with the shock tube wall heat-transfer measurements of Hartunian et al., which were made in the range $3 \leq M_s \leq 8$. Approximate analytical expressions for turbulent boundary-layer properties are deduced, and estimates of the wall temperature variation with distance behind the shock are given. Effects of blowing (wall ablation) are estimated. It is found that for strong shock waves wall blowing decreases, rather than increases, the vertical velocity at the edge of the boundary layer. The need for experimental data to confirm large Mach number and blowing effects predictions is noted.

Nomenclature

C_f, C_H	= local shear and heat-transfer coefficients, Eq. (1)
d	= tube diameter, ft
h	= static enthalpy per unit mass
h_e	= static enthalpy at edge of boundary layer, $h_i \{1 + [(\gamma - 1)/2] (1 - W^{-2}) M_s^2\}$
h_r	= recovery (adiabatic wall) value of h in laboratory coordinates, $h_e + [(\gamma - 1)/2] Pr^{1/2} (1 - W^{-1})^2 M_s^2 h_i$
ℓ_m	= distance between shock and contact surface in shock tube operating at maximum test time, ft (Ref. 2)
M_s	= shock Mach number, u_w/a_i
Pr	= Prandtl number
p	= pressure, atm
$-q_w$	= heat transfer to wall, $(k\partial T/\partial y)_w$
Re	= local Reynolds number, $\rho_e (u_w - u_e) x / \mu_e$
\bar{Re}_m	= equivalent flat plate Reynolds number at contact surface, $\rho_e u_e (W - 1)^2 \ell_m / \mu_e$. $\bar{Re}_m \geq 0(10^7)$ for turbulent boundary-layer estimate for ℓ_m to apply (Ref. 2)
T	= temperature, °R
u	= velocity in x direction, shock-fixed coordinates
u_w	= shock speed (wall velocity in shock-fixed coordinates)
u_e	= vertical velocity at edge of boundary layer
W	= u_w/u_e , ρ_e/ρ_i
x	= streamwise distance, ft
x_c	= boundary-layer closure station, Eq. (5c)
γ	= ratio specific heats
δ	= boundary-layer thickness
δ^*	= displacement thickness, shock-fixed coordinates,
	$\int_0^\infty [(1 - (\rho u / \rho_e u_e))] dy$
δ^{**}	= effective displacement thickness in blowing cases, Eq. (13)

θ = momentum thickness, shock-fixed coordinates,

$$\int_0^\infty (\rho u / \rho_e u_e) [1 - (u/u_e)] dy$$

μ = viscosity

ρ = density

τ_w = wall shear $(\mu \partial u / \partial y)_w$

Subscripts

e = freestream downstream of shock

r = recovery value

w = wall value downstream of shock

0 = zero wall blowing value

i = freestream value upstream of shock

Introduction

A PREVIOUS theory^{1,2} for turbulent boundary-layer development behind a shock moving with uniform speed has been re-examined with the objectives of facilitating the evaluation of the turbulent boundary-layer characteristics in air and estimating the effects of wall ablation in the case of strong shocks. The results are presented herein. In particular, numerical results for turbulent boundary-layer characteristics are tabulated, approximate analytic expressions are presented, wall surface temperature estimates are provided, and effects of ablation are deduced. Further details are provided in Ref. 3.

Theory

The turbulent boundary layer behind a shock moving with uniform speed in air is considered in shock-fixed coordinates. The flow (Fig. 1) is steady in this coordinate system. The nonblowing and blowing cases are considered separately.

Nonblowing Cases

Numerical Results

Numerical results, based on Refs. 1 and 2, for the turbulent boundary layer behind a shock propagating into real air,⁴ are given in Table 1. The computational procedure is outlined in Appendix A. Wall blowing effects are ignored. An initial air temperature $T_i = 522^\circ\text{R}$ is assumed. The results are only

Presented as Paper 83-0567 at the AIAA 21st Aerospace Sciences Meeting, Reno, Nev. Jan. 10-13, 1983, received March 25, 1983; revision received Sept., 2, 1983. Copyright © American Institute of Aeronautics and Astronautics, Inc., 1983. All rights reserved.

*Associate Laboratory Director, Aerophysics Laboratory. Fellow AIAA.

weakly dependent on T_l . Measurements of the turbulent heat transfer behind a shock propagating in air have been presented for shock Mach numbers in the range $3 \leq M_s \leq 8$ (Ref. 5). Comparison of these results (Fig. 2) with the heat-transfer predictions given in Table 1 shows good agreement (within a few percent of the experimental value at each shock Mach number). This agreement tends to confirm the theory of Refs. 1 and 2 for Mach numbers in the range $M_s \leq 10$ and nonblowing walls.

Approximate Analytic Expressions

Approximate analytic expressions for turbulent boundary-layer parameters have been deduced using the procedure outlined in Appendix B. The results for $T_l = 522^\circ \text{R}$ are

$$(p_1 x)^{1/5} \frac{\delta}{x} = 0.0370 \left\{ \frac{(W-1)^3}{[W + (7/3)]^4} \right\}^{1/5} \quad (1a)$$

$$(p_1 x)^{1/5} C_f = \frac{-2\tau_w (p_1 x)^{1/5}}{\rho_e (u_w - u_e)^2} = 2.22 \times 10^{-3} \left[\frac{W + (7/3)}{(W-1)^2} \right]^{1/5} \quad (1b)$$

$$(p_1 x)^{1/5} C_H = \frac{(-q_w) (p_1 x)^{1/5}}{\rho_e (u_w - u_e) (h_r - h_w)} = \frac{(p_1 x)^{1/5} C_f}{2Pr^{2/3}} \quad (1c)$$

$$(p_1 x)^{1/5} \frac{(-v_e)}{u_w - u_e} = 4.65 \times 10^{-3} \left\{ \frac{(W-1)^3}{[W + (7/3)]^4} \right\}^{1/5} \quad (1d)$$

$$(p_1 x)^{1/5} \left(\frac{-\delta^*}{x} \right) = \frac{5}{4} (W-1) \left[(p_1 x)^{1/5} \frac{(-v_e)}{u_w - u_e} \right] \quad (1e)$$

$$(p_1 x)^{1/5} \frac{(-\theta)}{x} = \frac{5}{8} (W-1)^2 \left[\frac{-2(p_1 x)^{1/5} \tau_w}{\rho_e (u_w - u_e)^2} \right] \quad (1f)$$

where x is in feet, p_1 is in atmospheres, and $W = u_w/u_e = \rho_e/\rho_1$ is the velocity (density) ratio across the shock. The quantities C_f , C_H , and v_e are normalized by the use of $u_w - u_e$, which is the freestream velocity in laboratory (wall stationary) coordinates. It is seen that v_e is negative, i.e., the vertical velocity at the edge of the boundary layer is directed toward the wall. This is the result of the aspirating effect of the wall in shock-fixed coordinates (Fig. 1). The quantities δ^* and θ are also negative in the present coordinate system, as can be seen from the relations

$$\frac{d\delta^*}{dx} = \frac{4}{5} \frac{\delta^*}{x} = \frac{v_e}{u_e}$$

$$\frac{d\theta}{dx} = \frac{4}{5} \frac{\theta}{x} = \frac{\tau_w}{\rho_e u_e^2}$$

which are alternatives to Eqs. (1e) and (1f). Equations (1) agree with the numerical results in Table 1 to within about 10%.

Surface Temperature Variation

The heat transfer to the wall, as a function of time after shock passage, has the form $-q_w \sim t^{-1/5}$. The departure of wall-surface temperature T_w from its initial value T_l can be found from⁶

$$T_w - T_l = \frac{(-q_w) t^{1/5}}{[\pi(\rho \bar{C} k)_b]^{1/2}} \int_0^t \frac{d\tau}{(t-\tau)^{1/5} \tau^{1/2}} = \frac{1.297(-q_w) t^{1/2}}{(\rho \bar{C} k)_b^{1/2}} \quad (2)$$

where $(\rho \bar{C} k)_b$ is the product of density, specific heat, and thermal conductivity of the wall ("body") material. Dependence of the latter properties on temperature is neglected. The variation of wall-surface temperature with distance behind the shock can be shown to equal (for strong shocks)

$$\frac{1}{p_1^{0.8} x^{0.3}} \left(\frac{T_w}{T_l} - 1 \right) = EM_s^{5/2} W^{4/5} \left[1 + O\left(\frac{1}{W}\right) \right] \quad (3)$$

where E is a function of wall material; typical values (from Carslaw and Jaeger⁶) are given in Table 2. The present theory is valid when the change in wall-surface temperature is small relative to the recovery temperature T_r . For strong shocks, the latter ratio is found from

$$\frac{1}{p_1^{0.8} x^{0.3}} \frac{T_w - T_l}{T_r} = \frac{E}{0.38} M_s^{1/2} W^{4/5} \left[1 + O\left(\frac{1}{W}\right) \right] \quad (4)$$

Equations (2-4) neglect ablation, which tends to limit the wall-surface temperature increase and, therefore, extend the region of validity of the present results. However, the effects of blowing on the boundary-layer properties need to be considered.

Shock Tube Application

The present results can be used to evaluate maximum test time and boundary-layer closure in high-pressure shock tubes that employ air as the driven (test) gas.

In a shock tube of diameter d , operating at its maximum test time, the separation between the contact surface and the shock is denoted by ℓ_m and is found from Ref. 2

$$\frac{1}{(p_1 d)^{1/4}} \frac{\ell_m}{d} = \frac{0.1768 W (W-1)}{W^2 + 1.25 W - 0.80} \left[(p_1 x)^{1/5} \left(\frac{-\delta^*}{x} \right) \right]^{-5/4} \quad (5a)$$

Values of ℓ_m are included in Table 1. The actual maximum test time is reduced somewhat because of mixing at the contact surface. Equation (5a) assumes that the boundary layer in the driven gas is turbulent. An equivalent flat plate Reynolds number, based on the distance that a freestream

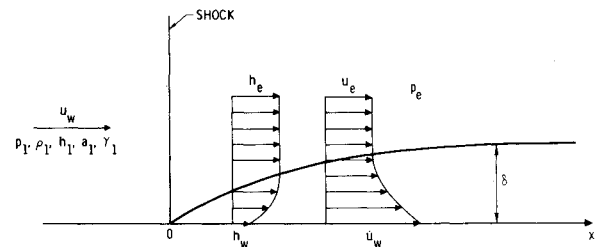


Fig. 1 Boundary layer behind shock in shock stationary coordinates.

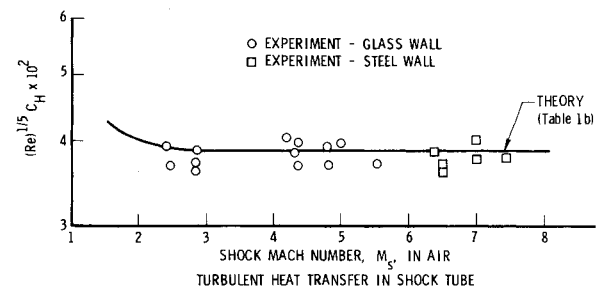


Fig. 2 Comparison of present theory with experimental data of Ref. 5.

Table 1 Turbulent boundary layer behind shock^a

M_s	W	T_e/T_l	$\frac{\delta^*/\delta}{1-W}$	$\frac{\theta/\delta}{1-W}$	$(p_1x)^{1/5}(\delta)/x$	$(p_1x)^{1/5}(-\delta^*)/x$	$(p_1x)^{1/5}(-\theta)/x$
1.01	1.0167	1.0066	0.1744	0.1256	0.001110	0.3234E-05	0.2330E-05
1.10	1.1691	1.0649	0.1698	0.1314	0.004312	0.1238E-03	0.9582E-04
1.20	1.3416	1.1280	0.1661	0.1378	0.006348	0.3602E-03	0.2987E-03
1.40	1.6897	1.2547	0.1614	0.1502	0.009060	0.1009E-02	0.9387E-03
1.60	2.0317	1.3880	0.1588	0.1623	0.010878	0.1782E-02	0.1822E-02
1.80	2.3592	1.5316	0.1572	0.1740	0.012190	0.2605E-02	0.2883E-02
2.00	2.6700	1.6900	0.1563	0.1851	0.013187	0.3442E-02	0.4076E-02
3.00	3.9500	2.6500	0.1549	0.2319	0.015849	0.7241E-02	0.1084E-01
4.00	4.8500	3.8500	0.1546	0.2655	0.016938	0.1008E-01	0.1732E-01
5.00	5.5500	5.3000	0.1541	0.2914	0.017534	0.1229E-01	0.2325E-01
6.00	6.1300	6.9500	0.1535	0.3124	0.017891	0.1409E-01	0.2867E-01
7.00	6.6500	8.7000	0.1528	0.3308	0.018109	0.1563E-01	0.3384E-01
8.00	7.2000	10.7000	0.1518	0.3496	0.018302	0.1723E-01	0.3968E-01
10.00	8.3000	14.3000	0.1501	0.3865	0.018435	0.2020E-01	0.5202E-01
12.00	9.0500	18.1000	0.1492	0.4117	0.018405	0.2210E-01	0.6099E-01
14.00	9.4000	22.4000	0.1489	0.4236	0.018323	0.2291E-01	0.6520E-01
16.00	9.9000	26.3000	0.1483	0.4402	0.018219	0.2405E-01	0.7137E-01
18.00	10.5500	29.7000	0.1476	0.4614	0.018095	0.2551E-01	0.7974E-01
20.00	11.1500	32.5000	0.1470	0.4810	0.017935	0.2676E-01	0.8756E-01

M_s	$\frac{1}{(p_1d)^{1/4}} \frac{x_c}{d}$	$\frac{1}{(p_1d)^{1/4}} \frac{\ell_m}{d}$	$\frac{1}{(p_1d)^{5/4}} \bar{Re}_m$	$(p_1x)^{1/5} C_f$	$(p_1x)^{1/5} C_H$	$Re^{1/5} C_H$	$\frac{(p_1x)^{1/5} (-v_e)}{W-1} \frac{1}{u_e}$
1.01	2.075E+3	0.1455E+05	0.2605E+08	0.01337	0.008321	0.0858	0.1549E-03
1.10	3.805E+2	0.1320E+04	0.2527E+09	0.00536	0.003337	0.0551	0.5858E-03
1.20	2.346E+2	0.6099E+03	0.4978E+09	0.00410	0.002550	0.0489	0.8436E-03
1.40	1.504E+2	0.2751E+03	0.9865E+09	0.00316	0.001965	0.0440	0.1170E-02
1.60	1.197E+2	0.1725E+03	0.1471E+10	0.00274	0.001705	0.0419	0.1382E-02
1.80	1.038E+2	0.1249E+03	0.1939E+10	0.00250	0.001554	0.0408	0.1533E-02
2.00	9.409E+1	0.9782E+02	0.2380E+10	0.00234	0.001456	0.0401	0.1649E-02
3.00	7.477E+1	0.4941E+02	0.4195E+10	0.00199	0.001241	0.0391	0.1964E-02
4.00	6.881E+1	0.3590E+02	0.5518E+10	0.00187	0.001163	0.0392	0.2095E-02
5.00	6.590E+1	0.2952E+02	0.6586E+10	0.00180	0.001118	0.0392	0.2162E-02
6.00	6.426E+1	0.2578E+02	0.7539E+10	0.00174	0.001085	0.0392	0.2197E-02
7.00	6.329E+1	0.2323E+02	0.8504E+10	0.00170	0.001056	0.0392	0.2213E-02
8.00	6.246E+1	0.2106E+02	0.9489E+10	0.00165	0.001028	0.0390	0.2223E-02
10.00	6.190E+1	0.1793E+02	0.1201E+11	0.00156	0.000972	0.0387	0.2214E-02
12.00	6.202E+1	0.1636E+02	0.1413E+11	0.00151	0.000937	0.0385	0.2196E-02
14.00	6.237E+1	0.1577E+02	0.1549E+11	0.00148	0.000920	0.0384	0.2182E-02
16.00	6.281E+1	0.1501E+02	0.1742E+11	0.00144	0.000897	0.0383	0.2162E-02
18.00	6.335E+1	0.1413E+02	0.1995E+11	0.00140	0.000871	0.0381	0.2137E-02
20.00	6.406E+1	0.1345E+02	0.2276E+11	0.00136	0.000846	0.0379	0.2109E-02

^a $Pr = 0.72$, $h_w = h_l$, $t_l = 522^\circ R$; p_1 is in atmospheres, x is in feet.

particle has moved relative to the wall, is $\bar{Re} = u_e(W-1)^2 x / \nu_e$. The value of \bar{Re} at the contact surface is

$$\frac{1}{(p_1d)^{5/4}} \bar{Re}_m = 6.93 \times 10^6 M_s \frac{\mu_1}{\mu_e} (W-1)^2 \left[\frac{\ell_m}{d} \frac{1}{(p_1d)^{1/4}} \right] \quad (5b)$$

Values of \bar{Re}_m are included in Table 1. Turbulent theory is applicable provided \bar{Re}_m is of the order 10^7 or greater.

Let x_c denote the distance behind the shock at which boundary-layer closure ($\delta = d/2$) occurs. This point separates the boundary-layer-type flow region ($0 < x < x_c$) from the fully developed pipe flow region ($x > x_c$). An estimate for x_c is obtained by letting $\delta = d/2$ in Eq. (1a). The result is

$$\frac{1}{(p_1d)^{1/4}} \frac{x_c}{d} = \left[2(p_1x)^{1/5} \frac{\delta}{x} \right]^{1/5} \quad (5c)$$

which is included in Table 1. Equation (5c) must be viewed as approximate, because transverse curvature effects and viscid-inviscid flow interaction are neglected. (These effects become important when δ/d is not small.) It is seen from Table 1 that $\ell_m/x_c < 1$ for $M_s > 2.0$ and $\ell_m/x_c > 1$ for $M_s < 2.0$. In the case when $M_s < 2.0$, boundary-layer closure is reached before the limiting separation is achieved and the solution for ℓ_m is generally not meaningful. In these cases, shock tube test time is determined by freestream uniformity requirements. In the case when $M_s > 2.0$ the limiting separation ℓ_m is reached before boundary-layer closure. In these cases, test time is determined by ℓ_m and the solution for x_c generally is not meaningful.

The above discussion of ℓ_m and x_c pertains to a conventional shock tube. An alternative situation is one wherein a strong shock (blast wave) is driven by an explosion with no distinction between driver and driven gas, i.e., there is no contact surface. A knowledge of the boundary-layer closure location is of interest for modeling of wall effects. In these

Table 2 Approximate thermal properties of the wall^a

	$(\rho \bar{C} k)_{\delta_0}^{1/2}$ cal/(cm ² K s ^{1/2})	E^b (atm) ^{-0.8} (ft) ^{-0.3}
Metal		
Aluminum	5.17×10^{-1}	3.92×10^{-4}
Mild steel (0.1% C)	3.19×10^{-1}	6.34×10^{-4}
Cast iron	3.48×10^{-1}	5.82×10^{-4}
Nonmetal		
Glass (crown)	3.67×10^{-2}	5.52×10^{-3}
Concrete (1:2:4)	3.41×10^{-2}	5.93×10^{-3}
Gas		
Air	1.34×10^{-4}	1.51×10^0

^a From Ref. 6. ^b $E = 2.024 \times 10^{-4} / (\rho \bar{C} k)_{\delta_0}^{1/2}$.

cases, Eq. (5c) may provide a useful estimate for x_c regardless of shock strength.

Wall Blowing Effect

The effect of blowing on wall shear and heat transfer is not well established for turbulent boundary layers. No experimental data are available for the case of a turbulent boundary layer behind a moving shock. Nevertheless, an estimate of this effect, based on results for semi-infinite flat plates, is presented herein. The blown gas is assumed to be air-like.

On the basis of the flat plate analogy,^{7,8} the ratio of blowing to nonblowing (subscript zero) shear and heat transfer can be expressed by

$$\frac{C_H}{(C_H)_0} = \frac{C_f}{(C_f)_0} = \frac{\ln(1+B')}{B'} \quad (6)$$

where

$$B' \equiv \frac{(\rho v)_w}{\rho_e |u_w - u_e| C_H} \equiv \frac{h_r}{\Delta H}$$

Here h_r is the recovery enthalpy in shock stationary coordinates (see Nomenclature) and $\Delta H \equiv -q_w / (\rho v)_w$ is the effective heat of ablation of the wall material. The value of B' readily can be estimated if the heat capacity of the unablated wall material is neglected. In the latter case, ΔH is the heat required to vaporize a unit mass of wall material which is initially at room temperature. For a vaporizing ($T = 3100$ K) steel wall, $\Delta H \approx 2100$ cal/g. As an example, consider a strong shock in air bounded by a steel wall. For air at an initial temperature of 290 K ($h_1 = 69.4$ cal/g), the recovery enthalpy behind a strong shock is $h_r = 0.38 M_s^2 h_1 = 26.4 M_s^2$. Thus, for the steel wall case, $B' = 5.0, 31$, and 126 for $M_s = 20, 50$, and 100 . Substitution of B' into Eq. (6) provides an estimate of the effect of wall blowing on wall shear and heat transfer.

The variation of boundary-layer momentum thickness with distance is of interest. The momentum integral equation can be expressed in the form

$$\frac{-1}{(W-1)^2} \frac{d\theta}{dx} = \frac{C_f}{2} + \frac{(\rho v)_w}{\rho_e u_e (W-1)} \quad (7)$$

Taking the Reynolds analogy to be $C_f = 2C_H$ and integrating, we obtain, at a fixed x ,

$$\frac{\theta}{\theta_0} = \frac{(1+B') \ln(1+B')}{B'} \quad (8)$$

from which momentum thickness can be obtained. The vertical velocity at the edge of the boundary layer is also of

interest. The latter can be expressed by

$$\frac{v_e}{u_e} = \frac{d\delta^*}{dx} + \frac{(\rho v)_w}{\rho_e u_e} \quad (9)$$

Assuming δ^*/δ_0^* is independent of x and recalling $d\delta_0^*/dx = (4/5)(\delta_0^*/x)$, we can express Eq. (9) as

$$\frac{v_e}{(v_e)_0} = \frac{\delta^*}{\delta_0^*} \times \left[1 - \frac{\ln(1+B')}{\frac{4}{5} \frac{\delta^*}{\delta_0^*} \left(\frac{\delta_0^*}{1-W} \right)} \frac{(p_1 x)^{1/5} (C_H)_0}{(p_1 x)^{1/5} \frac{\delta_0}{x}} \right] \quad (10)$$

The ratio δ^*/δ_0^* is needed. Figure 36 in Ref. 8 indicates that the form factor δ^*/θ is relatively insensitive to the blowing parameter B' . It can then be assumed that, at a fixed x ,

$$\frac{\delta^*}{\delta_0^*} = \frac{\delta}{\delta_0} = \frac{\theta}{\theta_0} = \frac{(1+B') \ln(1+B')}{B'} \quad (11)$$

The validity of Eq. (11) requires further study. Substitution into Eq. (10) then yields, for air,

$$\frac{v_e}{(v_e)_0} = \frac{(1+B') \ln(1+B')}{B'} \left[1 - \frac{0.256 B'}{1+B'} \left(\frac{W + (7/3)}{W-1} \right) \right] \quad (12a)$$

$$= \frac{(1+0.744 B') \ln(1+B')}{B'} \quad \text{for } W \gg 1 \quad (12b)$$

For strong shocks, $W \gg 1$, the ratio $v_e/(v_e)_0$ is increased by wall blowing. Since $(v_e)_0$ is negative, the latter result indicates that wall blowing decreases rather than increases the vertical velocity at the edge of the boundary layer, i.e., v_e becomes more negative as wall blowing, $(\rho v)_w$, increases. This somewhat surprising result is due to the momentum defect, associated with the wall blowing, which causes a more rapid rise in boundary-layer thickness and, therefore, a more rapid ingestion of freestream flow into the boundary layer.

Let δ^{**} correspond to the effective wall displacement thickness that corresponds to the boundary-layer edge velocity v_e for blowing cases. Thus,

$$\frac{d\delta^{**}}{dx} \equiv \frac{v_e}{u_e} \quad (13a)$$

$$\delta^{**} = \delta^* + \int_0^x \frac{(\rho v)_w}{\rho_e u_e} dx \quad (13b)$$

In the absence of blowing, $\delta_0^{**} = \delta_0^*$. Since all boundary-layer thicknesses vary such as $x^{4/5}$ for both blowing and nonblowing cases, it follows that at a fixed x location,

$$\frac{\delta^{**}}{\delta_0^{**}} = \frac{v_e}{(v_e)_0} \quad (14)$$

In the case of blowing, δ^* in Eq. (5a) should be replaced by δ^{**} . It follows that the effect of blowing on test time is given by

$$\frac{\ell_m}{(\ell_m)_0} = \left(\frac{\delta^{**}}{\delta_0^{**}} \right)^{-5/4} \quad (15)$$

which is evaluated using Eqs. (12) and (14). The effect of blowing on boundary-layer closure, however, is obtained

from Eqs. (5c) and (11):

$$\frac{x_c}{(x_c)_0} = \left[\frac{(1+B') \ln(1+B')}{B'} \right]^{-5/4} \quad (16)$$

For the previous example of a strong shock in air bounded by a steel wall, $\ell_m/(\ell_m)_0 = 0.52, 0.29, 0.20$, and $x_c/(x_c)_0 = 0.38, 0.20, 0.14$ for $M_s = 20, 40, 100$, i.e., for $B' = 5, 31, 126$.

Concluding Remarks

The present results are intended to facilitate estimates of the turbulent boundary layer behind shocks moving in air. The results are expected to be fairly accurate for nonblowing walls and for $M_s \leq 0(10)$ (e.g., Fig. 2). Further study is required for validation of the results for $M_s > 10$ and a nonblowing wall. Effects of blowing can be considered uncertain for all M_s . Further comparisons with experiment, and comparisons with numerical results from more accurate turbulent boundary-layer codes, are desirable for $M_s > 10$ and for wall blowing.

Appendix A: Method of Solution

The procedure for obtaining numerical estimates for turbulent boundary-layer properties, based on Refs. 1 and 2, is outlined herein.

The flow is considered in shock-fixed coordinates (Fig. 1). Boundary-layer profiles are approximated by

$$\frac{u_w - u}{u_w - u_e} = \zeta^{1/7} \quad (A1a)$$

$$\frac{\rho_e}{\rho} = \frac{h}{h_e} = 1 + b\zeta^{1/7} - c\zeta^{2/7} \quad (A1b)$$

where $\zeta = y/\delta$ and

$$b = (h_r/h_w) - 1 \quad (A2a)$$

$$c = (h_r/h_w) - (h_e/h_w) \quad (A2b)$$

$$\frac{h_r}{h_e} = 1 + \frac{r(0)}{2} \frac{(W-1)^2 u_e^2}{h_e} \quad (A2c)$$

Here $r(0)$ is the recovery factor. The wall is assumed to remain at its original temperature (i.e., $h_w = h_l$), and the ratio h_e/h_l is obtained from shock relations. Momentum and displacement thicknesses are found by substitution of Eqs. (A1) and (A2) into

$$\frac{\theta}{\delta} = \int_0^1 \frac{\rho u}{\rho_e u_e} \left(1 - \frac{u}{u_e}\right) d\zeta \quad (A3a)$$

$$\frac{\delta^*}{\delta} = \int_0^1 \left(1 - \frac{\rho u}{\rho_e u_e}\right) d\zeta \quad (A3b)$$

Shear and boundary-layer thickness are related by the Blasius relation

$$\frac{\tau_w}{\rho_m (u_w - u_e)^2} = 0.0225 \left[\frac{v_m}{(u_w - u_e) \delta} \right]^{1/4} \quad (A4a)$$

where subscript m denotes evaluation at a mean enthalpy given by

$$h_m = 0.5(h_w + h_e) + 0.22(h_r - h_e) \quad (A4b)$$

Equations (A1-A4) permit solution of the momentum integral equation

$$\frac{\tau_w}{\rho_e u_e^2} = \frac{d\theta}{dx} = \frac{4}{5} \frac{\theta}{x} \quad (A5a)$$

for θ and τ_w . Heat transfer is obtained from

$$\frac{Pr^{2/3} (W-1)}{\rho_e u_e (h_r - h_w)} q_w = \frac{\tau_w}{\rho_e u_e^2} \quad (A5b)$$

All other boundary-layer properties can be deduced readily.

For the present case of shock propagating in air, assume $\gamma_l = 7/5$, $Pr = 0.72$, $r(0) = 0.90$, $T_w = T_l = 522^\circ\text{R}$,† and $h_w = h_l$. Corresponding values of M_s , $W = u_w/u_e = \rho_e/\rho_w$, and T_e/T_l are found from real gas⁴ shock relations. Noting $0.7 \leq (h_m/h_e) \leq 1.0$, we assume further that $T_m/T_l = (h_m/h_e)(T_e/T_l)$ and $\rho_m/\rho_e = h_e/h_m$, where h_m/h_e is found from Eqs. (A4) and

$$\frac{h_e}{h_l} = 1 + 0.2M_s^2 \left(1 - \frac{1}{W^2}\right) \quad (A6a)$$

$$\frac{h_r}{h_e} = 1 + \frac{0.18M_s^2}{h_e/h_l} \left(\frac{W-1}{W}\right)^2 \quad (A6b)$$

For air at $T_l = 522^\circ\text{R}$

$$\left(\frac{\rho a}{p\mu}\right)_l = 6.93 \times 10^6 (\text{atm-ft})^{-1} \quad (A7)$$

where p_l is in atmospheres. The Sutherland relation for the viscosity of air is used, namely,

$$\frac{\mu}{\mu_l} = \left(\frac{T}{T_l}\right)^{3/2} \frac{T_l + 198.6}{T + 198.6} \quad (A8)$$

where T is in degrees Rankine. Boundary-layer properties readily can be found. For example, the boundary-layer thickness is obtained from

$$(p_l x)^{1/5} \frac{\delta}{x} = 2.46 \times 10^{-3} \left[\left(\frac{1-W}{\theta/\delta}\right)^4 (W-1)^3 \left(\frac{h_e}{h_m}\right)^3 \frac{\mu_m/\mu_l}{M_s} \right]^{1/5} \quad (A9)$$

The numerical results for all boundary-layer properties are listed in Table 1.

Appendix B: Approximate Analytic Formulation

Approximate analytic expressions for boundary-layer properties can be obtained by use of the approximate expressions for Eqs. (A3) presented in Ref. 2. For ideal gases, the latter are

$$\frac{\theta/\delta}{1-W} = \frac{3W+7}{80} \quad \gamma = 7/5 \quad (B1a)$$

$$\frac{\delta^*/\delta}{1-W} = 0.157 \quad \gamma = 7/5, W \geq 2 \quad (B1b)$$

Equations (B1a) and (B1b) are correct to within 8% for strong shocks in air with $W \leq 15$.

Consider the case of a strong shock moving into air. Neglecting terms of order $1/M_s^2$, $1/W$, and h_w/h_e compared with 1, we find $h_e/h_l = 0.2M_s^2$, $h_r/h_e = 1.9$, and $h_m/h_e = 0.700$. Also, for $T_l = 522^\circ\text{R}$ and $198.6/T_m \ll 1$, the Sutherland relation becomes $\mu_m/\mu_l = 1.380 (T_m/T_l)^{1/2}$. Then, if it is assumed that $T_m/T_l = h_m/h_l = 0.14M_s^2$, the

†The solution is relatively insensitive to the assumption $T_l = 522^\circ\text{R}$. For $\mu \sim T^\omega$, it can be shown that $\delta \sim T_l^{0.2\omega+0.1}$.

viscosity law becomes $\mu_m/\mu_l = 0.524M_s$. Substitution of the relations

$$\mu_m/\mu_l = 0.524M_s \quad h_m/h_e = 0.700 \quad (B2)$$

and Eq. (B1a) into Eq. (A9) yields,

$$(p_1 x)^{1/5} \frac{\delta}{x} = 0.0370 \left\{ \frac{(W-1)^3}{[W+(7/3)]^4} \right\}^{1/5} \quad (B3)$$

Equation (B3) is in remarkably good agreement with all of the numerical results in Table 1, including W near 1, since δ/x is relatively insensitive to the approximations used to obtain Eq. (B2). Equation (B3) agrees with the results in Table 1 to within 10%. Hence, all boundary-layer properties of interest can be deduced from Eqs. (B1) and (B3) with an accuracy of about 10%. The corresponding analytic expressions are given by Eqs. (1).

Acknowledgment

This work was supported by the U.S. Air Force under Space Division Contract F04701-82-C-0083.

References

- ¹Mirels, H., "Boundary Layer Behind Shock or Thin Expansion Wave Moving into Stationary Fluid," National Advisory Committee for Aeronautics, Washington, D.C., TN 3712, May 1956.
- ²Mirels, H., Shock Tube Test Time Limitation due to Turbulent-Wall Boundary Layer," *AIAA Journal*, Vol. 2, Jan. 1964, p. 84.
- ³Mirels, H., "Estimates of Turbulent Boundary Layer Behind a Shock Wave Moving with Uniform Velocity," The Aerospace Corp., El Segundo, Calif., TR-0078(3781-02)-1, Dec. 1977.
- ⁴Lewis, C. H., Burgess III, E. G., "Charts of Normal Shock Wave Properties in Imperfect Air," Arnold Engineering Development Center, Air Force Systems Command, Arnold Air Force Station, Tenn., AEDC-TDR-64-43, March 1964; also "Charts of Normal Shock Wave Properties in Imperfect Air (Supplement: $M_s = 1$ to 10)," Arnold Engineering Development Center, Air Force Systems Command, AEDC-TR-65-196, Sept. 1965.
- ⁵Hartunian, R. A., Russo, A. L., and Marrone, P. V., "Boundary-Layer Transition and Heat Transfer in Shock Tubes," *Journal of the Aerospace Sciences*, Vol. 27, Aug. 1960, p. 587.
- ⁶Carslaw, H. S. and Jaeger, J. C., *Conduction of Heat in Solids*, Oxford University Press, London, 1959, pp. 76, 496.
- ⁷Dorrance, W. H., *Viscous Hypersonic Flow*, McGraw-Hill Book Co., New York, 1962, pp. 59, 206-220.
- ⁸Kays, W. M. and Moffat, R. J., "The Behavior of Transpired Turbulent Boundary Layers," *Studies in Convection*, edited by B. E. Launder, Academic Press, New York, 1975, p. 251.

From the AIAA Progress in Astronautics and Aeronautics Series

THERMOPHYSICS OF ATMOSPHERIC ENTRY—v. 82

Edited by T.E. Horton, The University of Mississippi

Thermophysics denotes a blend of the classical sciences of heat transfer, fluid mechanics, materials, and electromagnetic theory with the microphysical sciences of solid state, physical optics, and atomic and molecular dynamics. All of these sciences are involved and interconnected in the problem of entry into a planetary atmosphere at spaceflight speeds. At such high speeds, the adjacent atmospheric gas is not only compressed and heated to very high temperatures, but strongly reactive, highly radiative, and electronically conductive as well. At the same time, as a consequence of the intense surface heating, the temperature of the material of the entry vehicle is raised to a degree such that material ablation and chemical reaction become prominent. This volume deals with all of these processes, as they are viewed by the research and engineering community today, not only at the detailed physical and chemical level, but also at the system engineering and design level, for spacecraft intended for entry into the atmosphere of the earth and those of other planets. The twenty-two papers in this volume represent some of the most important recent advances in this field, contributed by highly qualified research scientists and engineers with intimate knowledge of current problems.

544 pp., 6 × 9, illus., \$30.00 Mem., \$45.00 List

TO ORDER WRITE: Publications Order Dept., AIAA, 1633 Broadway, New York, N.Y. 10019